Results of Experimental Study of Hollow Cathodes in High Current Plasma Discharge

IEPC-2009-224

Presented at the 31st International Electric Propulsion Conference,
University of Michigan • Ann Arbor, Michigan • USA
September 20 – 24, 2009

Ryan T. Downey[1] and Paul Giuliano[2],
[1]*University of Southern California, Los Angeles, CA 90089, USA*
[2]*University of Michigan, Ann Arbor, Michigan 48109, USA*

Keith Goodfellow[3],
University of Southern California, Los Angeles, CA 90089, USA

and

Dan Erwin[4]
University of Southern California, Los Angeles, CA 90089, USA

Abstract: This paper presents an excerpt of data from recent research at the University of Southern California addressing several concerns of the mechanisms controlling performance and lifetime of high-current single-channel-hollow-cathodes, the central electrode and primary life-limiting component in magnetoplasmadynamic thrusters. Specifically covered are the trends seen in the discharge efficiency and power, the size of the plasma attachment to the cathode (the active zone), cathode exit plume plasma density and energy, along with plasma property distributions of the internal plasma column (the IPC) of a single-channel-hollow-cathode. Employing tantalum cathodes of 2 mm inner diameter, experiments were conducted to measure the axial temperature profile of operating cathodes, the width of the active zone, the discharge voltage and power, plasma arc resistance and efficiency, with mass flow rates of 50 to 300 sccm of argon, and discharge currents of 15 to 50 Amps. Langmuir probing was employed to obtain measurements for the electron temperature, plasma density and plasma potential at the cathode exit plane (down stream tip). Comparisons of results with previous similar studies of hollow cathodes conducted in a vaporized lithium medium are discussed.

I. Introduction

Electric propulsion (EP) systems are a clear and reliable choice to meet present and future in-space propulsion needs for high efficiency propulsion. Electric propulsion thrusters apply direct force to ionized gas via electric and magnetic fields to produce directed thrust. By these means, EP thrusters are capable of achieving specific impulses in the thousands of seconds, thus reducing the amount of propellant necessary to achieve mission propulsion goals.

For large-scale missions requiring both highly efficient propulsion systems and relatively high thrust levels, the Lorentz Force Accelerators (LFA) is a suitable candidate. LFA thrusters are notable among the cadre of EP systems for their capability of producing thousands of seconds of I_{sp} while providing 10's to 100's of Newton's of thrust, and have an extremely high power processing density. Additionally the efficiency of LFA thrusters scales with the thruster power making them particularly suitable for high power missions.

---

[1] Doctoral candidate, Astronautics and Space Technology Division, downey@usc.edu

[2] Graduate Student, Department of Aerospace Engineering, pgiulian@umich.edu

[3] Lecturer, Astronautics and Space Technology Division, goodfell@usc.edu

[4] Professor, Astronautics and Space Technology Division, Erwin@usc.edu

LFA thrusters are electromagnetic propulsion systems, producing a quasi-neutral exhaust plume, thus requiring no neutralizer to prevent spacecraft charging. The basic thruster design consists of a central cylindrical cathode typically made of tungsten (often doped with thorium), inside a larger annular shaped anode, also constructed of tungsten. An electrically neutral gas flows to fill the inter-electrode region where it will be ionized and accelerated downstream. Typical laboratory experiments use argon, while state-of-the-art flight system designs use vaporized lithium. The gas is initially ionized with a high voltage supply, after which point a high current supply is engaged to maintain the discharge. The erosion of the cathode material during both the startup and operational phases has been identified as the primary life limiting factor of LFA thrusters. This material erosion is directly controlled by material temperatures [7].

In addition to the cathode erosion, the other significant cathode mechanism strongly controlled by temperature is the thermionic emission of electrons from the material surface. This emission is governed by the well known Richardson equation for thermionic emission:

$$j = AT_{wall}^2 e^{-\phi_{eff}/k_b T_{wall}} \quad , \quad \phi_{eff} = \phi_{wf} - \sqrt{\frac{qE_s}{4\pi\varepsilon_o}} \tag{1}$$

Where j is the emitted surface current density in A/m^2, A is known as the Richardson coefficient, (6x10^5 A/m^2/K for tungsten), Φ_{wf} is the work function (in eV) of the material (= 4.5 for pure tungsten), and Φ_{eff} is the effective work function, which is an effective reduction of the work function by an applied electric field over the surface of the material, the *cathode sheath*. It is clear to see that the electron current emitted from the surface of a hot cathode is very sensitive to both temperature and work function, with the latter the dominant parameter.

A. Experiment

The experiment was conducted at the University of Southern California's Spacecraft Propulsion Lab, in the Astronautics and Space Technology division [1]. A Leeds and Northrup Disappearing Filament Optical Pyrometer (model # 8622-C) was used to obtain axial temperature profiles for the cathodes during operation with 2 mm spatial resolution. A Langmuir probe was employed to obtain plasma data at the downstream exit plane of the cathode. The probe consisted of a 0.25 mm diameter tungsten wire covered by a non-conducting ceramic tube, leaving 2 millimeters of the wire exposed to the plasma. The probe was attached to the end of a fast acting pneumatic linear actuator, which moves a shaft at a speed of 0.55 m/s a total of 500 mm. The high speed of the pneumatic linear actuator is necessary to ensure a small resonance time of the probe in the dense plasma region. For the plasma in these experiments the Debye length was on the order of 10^{-6} m, and the probe was sized such that the ratio of probe dimension to Debye length was ~10^3 m, thus the small plasma sheath analysis model is appropriate. Once introduced into the plasma, the probe was biased from -50 to +50 volts; Plasma probe data was measured and recorded with a Tektronix TDS 644A oscilloscope.

The cathodes used for the data in this paper were made of tantalum, and measured 38 mm in length, 3.22 mm outer diameter, 2.0 mm inner diameter, 0.6 mm wall thickness with a 0.5 mm long taper at the downstream end. Addition tungsten cathodes were used in the experiment, measuring 6mm in inner diameter, with 0.5 mm wall thickness by approximately50 mm length, though limited useful data was obtained from these prior to failure. The plasma arc discharge was maintained with an EMS 10-250 high current supply from Lambda. All runs used argon as the working medium, with mass flow rates from 50 to 300 sccm, and discharge currents of 15 to 50 Amps. Once the high current arc was established and the thermal effects settled to steady state, axial temperature profiles were measured with the optical pyrometer, starting at the down stream tip, moving upstream at 2mm intervals until the end of the region of interest was reached. This procedure was repeated 3 times and the data points were averaged.

The linear actuator was engaged to position the center of the Langmuir probe tip on the exit plane of the cathode, coaxially. Once in position, the bias voltage was pulsed, and the current through the probe was read via the voltage drop across a shunt resistor via the oscilloscope, and stored for later analysis.

II. Results and Discussion

It is important to note that in the graphs, data is presented as a function of mass flow rate. Mass flow rate is a convenient measurement for the experimenter, but the relevant parameter is the gas density in the interior of the cathode, which (with all other parameters remaining constant) is a function of the mass flow rate. It is worth noting that interior gas density may also be controlled by varying the geometry of the cathode, which was not done in this study, and that the gas density has both axial and radial gradients inside the cathode.

Figure 1 shows the total discharge power as a function of mass flow rate at constant discharge current. From these graphs notice that there is a minimum discharge power necessary to maintain the arc at a constant discharge

current, thus there is a maximum in the discharge efficiency. Since the thrust of an MPD thruster is primarily dependant upon the discharge current, there is therefore a minimum voltage and power necessary for a desired thrust level, controlled by the gas density inside the cathode.

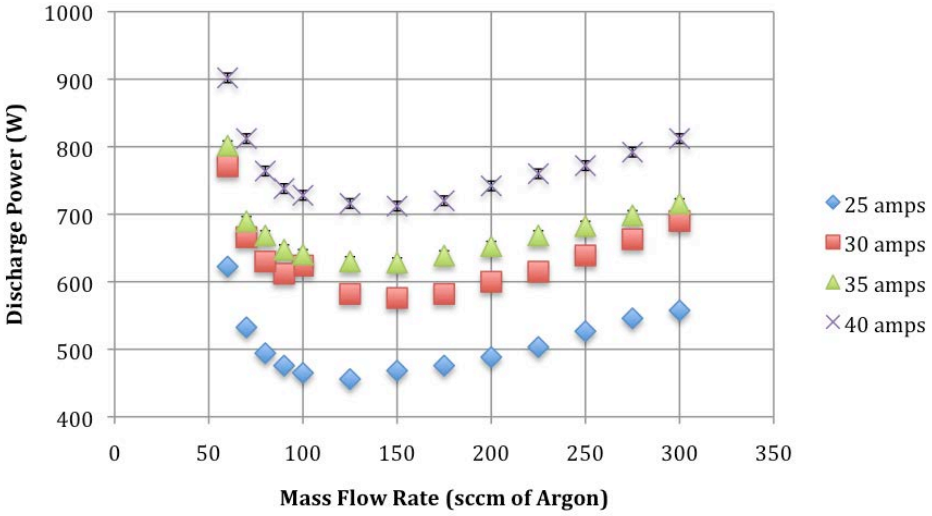

Figure 1: Total discharge power vs. mass flow rate.

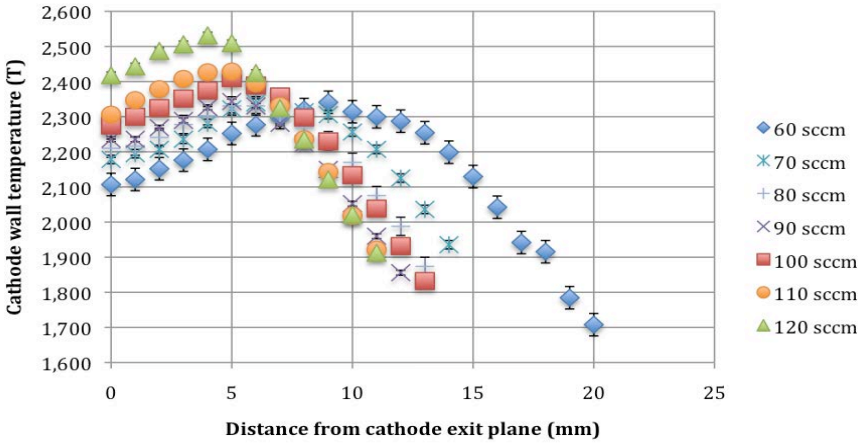

Figure 2: Axial temperature profiles at 25 amp discharge.

Figure 2 shows a representative sample of the data gathered for temperature profiles of the active cathode. From these plots the effects of the mass flow rate and discharge current on the temperature profiles are identifiable. The location of peak temperature in the cathode is some distance upstream from the exit plane of the cathode. Increased mass flow rates will raise the density of neutral gas inside the cathode and increasing the gas density yields peak temperatures further downstream (closer to the exit plane), and higher values of peak temperature. With time the cathode wall will thin due to evaporation, the most pronounced effects seen in the region of the hot spot, eventually vaporizing enough cathode material to open a hole in the wall, possibly causing failure of the cathode. The results of this effect can be seen in Figure 3, where a 6mm cathode is displayed following the erosion of an oval shaped hole measuring 4 mm by 3 mm in the cathode wall – the wall thinning at the axial location of the hot spot was severe enough that the cathode cracked during post test handling.

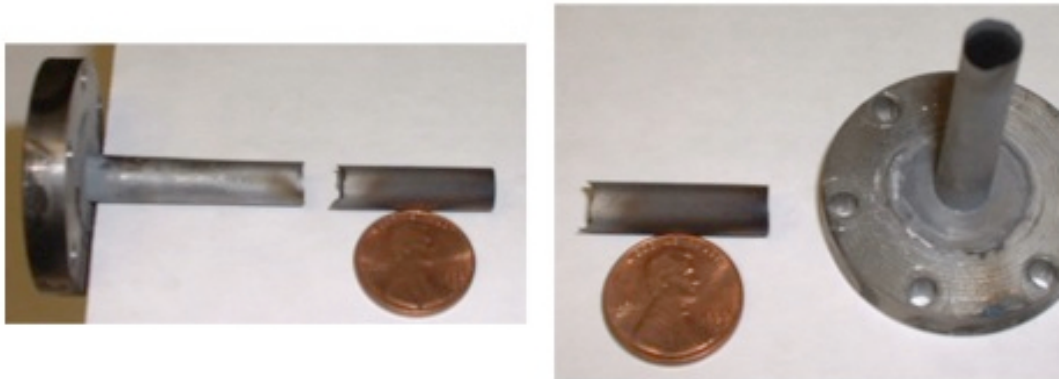

Figure 3: Failure of 6mm diameter tungsten cathode

Previous studies of similar nature using solid rod cathodes [8] exhibited the same trends in both temperature profiles and cathode erosion. Figure 4 shows the damage to a solid rod cathode as part of a study at the University of Stuttgart, in which the most significant damage was seen to both the cathode exterior and interior at a distance upstream of the cathode exit plane – the point of most significant damage is typically seen at the location of peak temperature. Figure 5 shows plots of axial temperature profiles of a thorium doped solid tungsten rod from previous work at JPL [8], in which the peak temperatures are seen upstream of the cathode tip. Increasing the background pressure of the chamber through variation of the mass flow rate was also seen to move the peak temperature further downstream. This trend is seen in orificed hollow cathodes, where the interior cathode pressure is kept relatively high due to the orifice place. In these cathodes, the peak temperature is always seen at the downstream limit of the cathode, as seen in the temperature profiles of the NSTAR cathode in Figure 6.

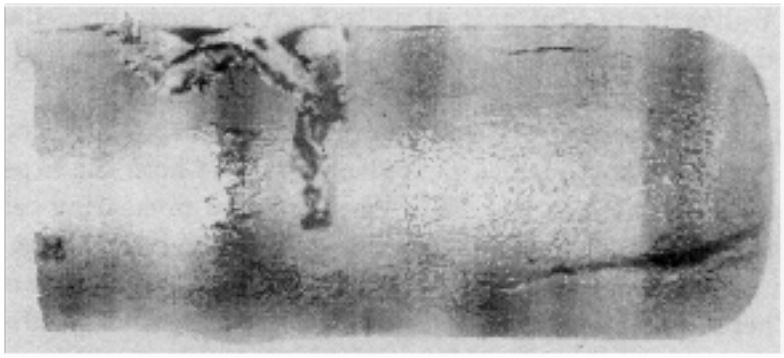

Figure 4. Damage seen in solid rod cathode, University of Stuttgart ZT1 thruster. Reference [8].

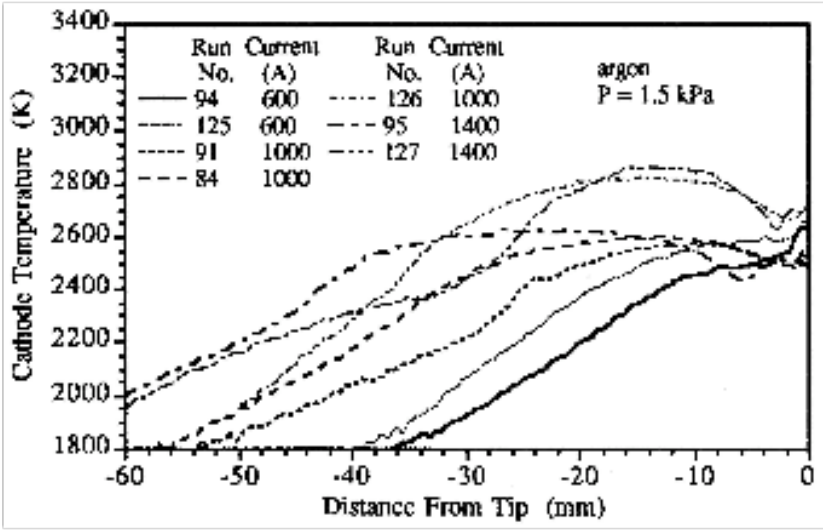

Figure 5. Axial temperature profiles of a thoriated tungsten solid rod cathode. Reference [8].

Note that this effect can also be seen in orificed hollow cathodes [3, 4], which maintain a relatively high and homogenous pressure inside the cathode. In orificed hollow cathodes the peak temperature is always seen at the very downstream limit of the cathode. The high gas density inside the orificed hollow cathodes makes them analogous to running an open ended hollow cathode at high flow rates.

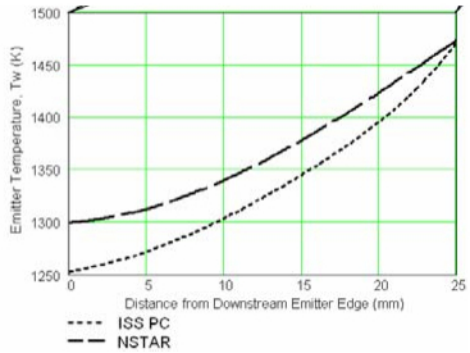

Figure 6. Temperature profile of orificed hollow cathode. Reference [4]

To make this relation more clear, picture raising the flow rate of the open ended cathode, moving the peak temperature further downstream and seeing the density of the gas inside the cathode continuously rise. Eventually the interior density would rise to a point at which the location of peak temperature would move all the way downstream to the tip of the cathode, and the wall temperature profile of the open ended cathode would resemble that of the orificed cathode.)

While at constant discharge current, the temperature of the cathode at the exit plane (cathode tip temperature) is seen to increase with increasing flow rate.

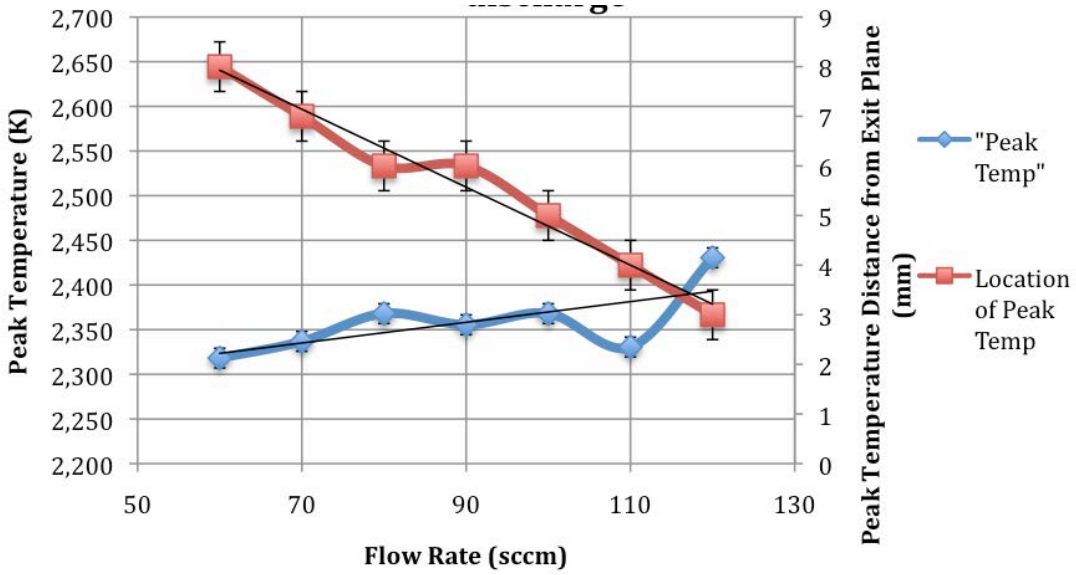

Figure 7: Location and magnitude of the peak temperature, vs. mass flow rate, 20 amp discharge

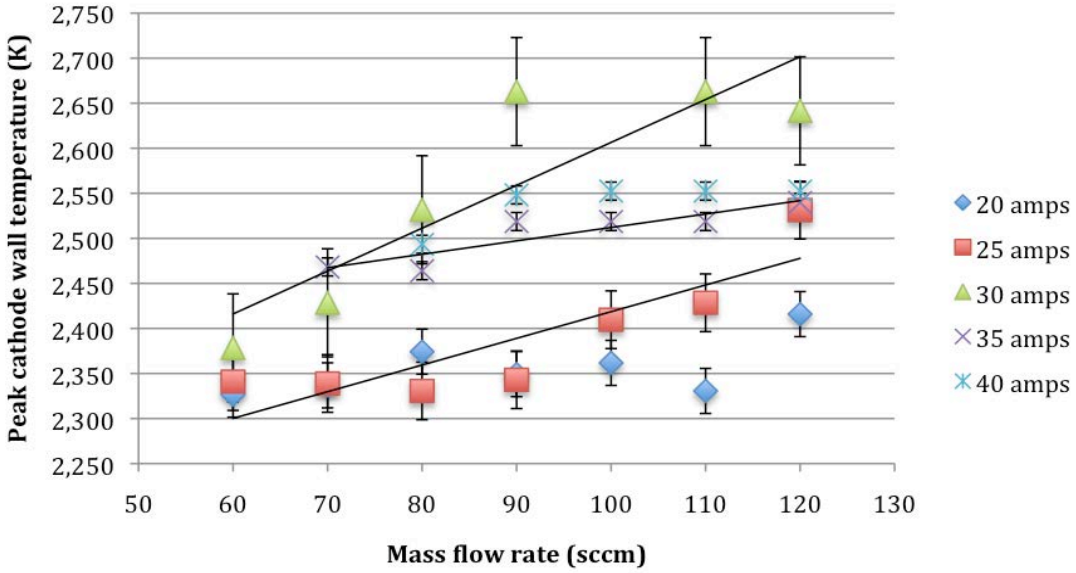

Figure 8: Peak cathode wall temperature vs. mass flow rate, with discharge current as parameter

From Figure 7 and Figure 8 the magnitude of the peak cathode wall temperature does show a slight dependence upon the mass flow rate, with the peak temperature increasing with increasing flow rate. This trend is in contradiction with reports of previous similar studies [5, 6] which concluded the peak temperature has no dependence upon mass flow rate. This result identifies a significant role that the interior cathode gas density plays in controlling the lifetime of the cathode - even a slight trend in temperature can be very important due to the thermionic emission current density's extreme sensitivity to surface temperature. Reduction of the peak temperature while keeping the discharge constant is a key goal of achieving increased cathode lifetime.

For this analysis the active zone has been defined as the region of cathode wall responsible for 75% of the total thermionic emission of electrons from the cathode (note that there is no standard for defining the physical limits of the active zone). Further, as this analysis was designed to yield qualitative results, only emission from the exterior cathode surface was considered. This decision was as result of a lack of reliable data for the sheath drop profile along the interior cathode surface. The voltage across the sheath will increase the thermionic emission from the cathode interior surface, through the Shotkey effect. Rather than including errors by attempting to make predictions of the Shotkey effect, it was decided to ignore interior thermionic emission and the Shotkey effect altogether and focus on exterior temperature profiles only, thus yielding a strongly qualitative analysis. As a result of

the construct of the analysis, the actual width of the active zone is understood to be smaller than the values shown in the plots.

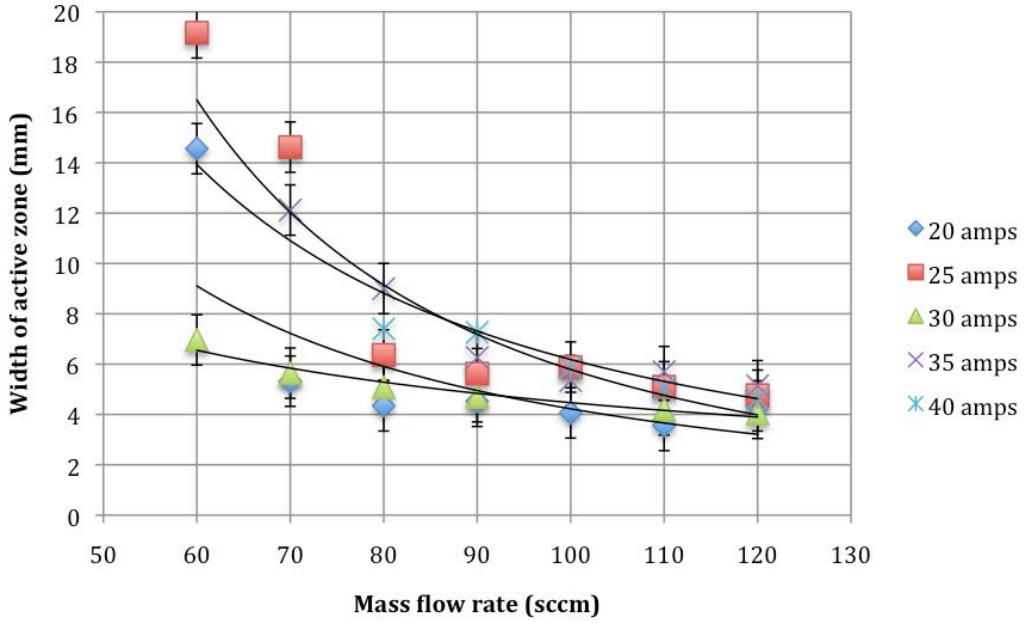

Figure 9. Width of Active Zone at 75% of total current, vs. mass flow rate

As can be seen in Figure 9 and Figure 10, the width of the active zone of the cathode is a function of both flow rate and discharge current. Reasonable trend lines show the width of the active zone to be a weakly increasing function of discharge current, and a decreasing function of the mass flow rate. One can see from Figure 8 that for a constant current the peak cathode wall temperature decreases with decreasing mass flow rate - to account for the corresponding loss in thermionic current emission, the width of the active zone will increases (and thus the temperature of the surrounding area will increase, flattening out the wall temperature profile).

The width of the active zone shows a dependence upon the discharge current, as seen in Figure 10 with a doubling of the discharge current increasing the active zone width by approximately 50%. A reduction in the mass flow rate through the cathode results in an increase in the width of the active zone. Reducing the mass flow rate will decrease the plasma density. This decrease in plasma density means that the total number of ions near the wall available to fall through the sheath and deposit energy to the wall has decreased, and this corresponds to an increase in the area over which the plasma needs to "attach" to the wall and the ions deposit energy from wall strikes. The result is the location of peak temperature moves further upstream and the region of plasma attachment to the cathode wall increases. Data on the variance of the profile of the sheath drop across the cathode as it varies with mass flow and discharge current is required for any quantitative analysis of the active zone.

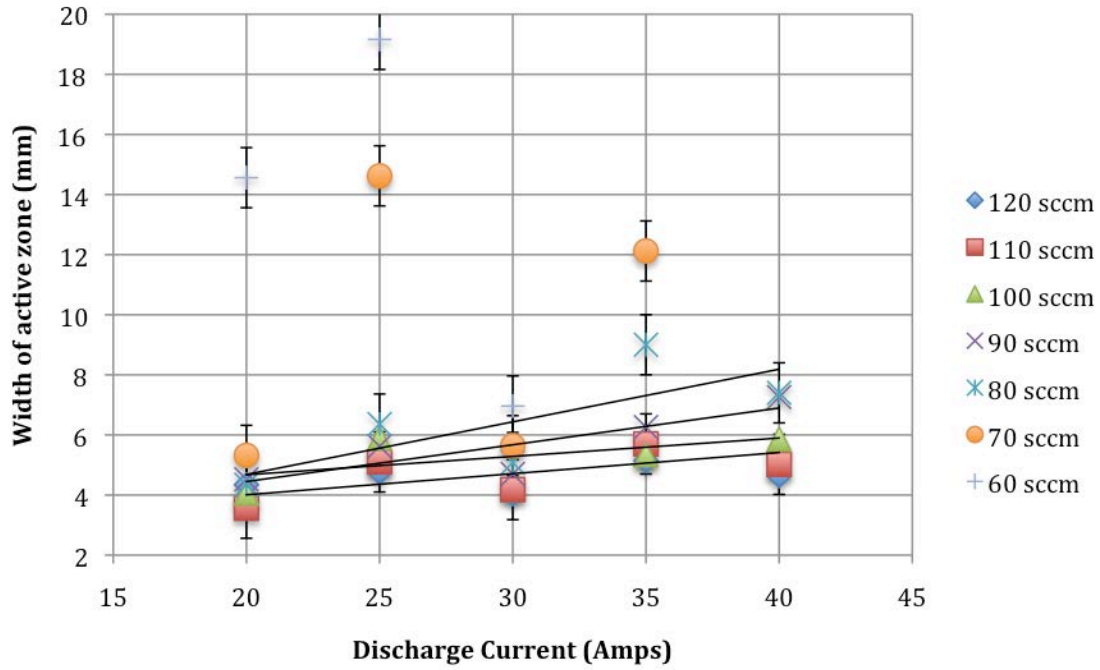

Figure 10. Width of Active Zone at 75% of total current, vs. the discharge current

Electron temperature and number densities were experimentally collected by Langmuir probing at a point 1 cm downstream from the cathode exit plane, on the cathode centerline. At this location the electrons have undergone many collisions, and are expected to be well thermalized. A plot of the electron temperature as a function of the mass flow rate and discharge current can be seen in Figure 11 and Figure 12 respectively. The effects of the mass flow rate and discharge current on the plasma density are shown in Figure 13 and Figure 14.

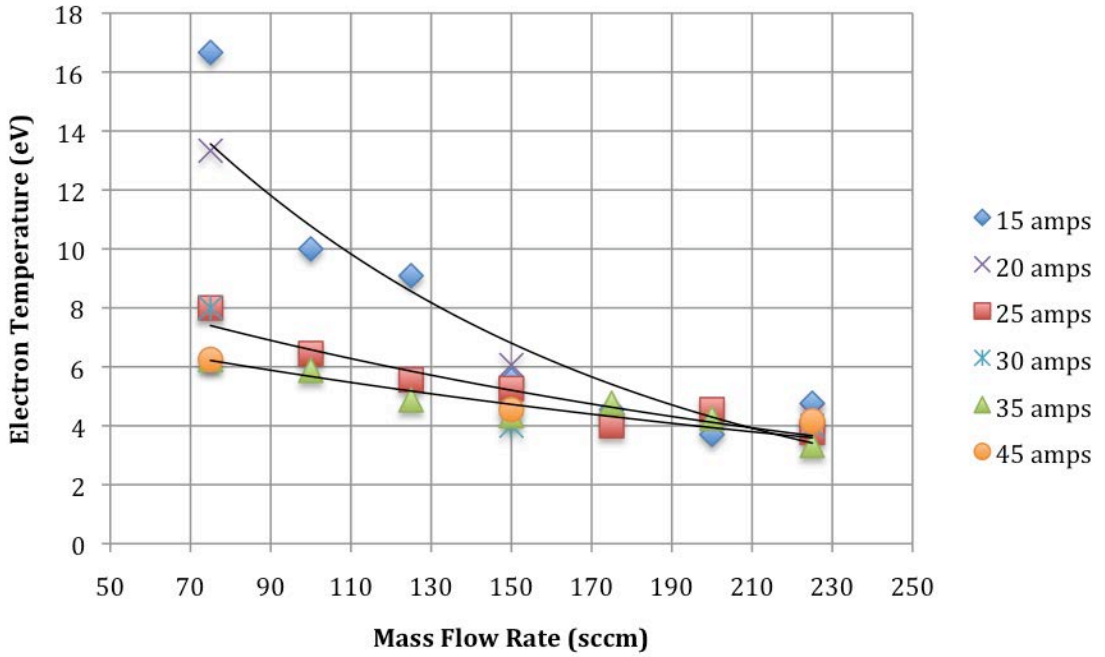

Figure 11: Electron temperature vs. Mass flow rate.

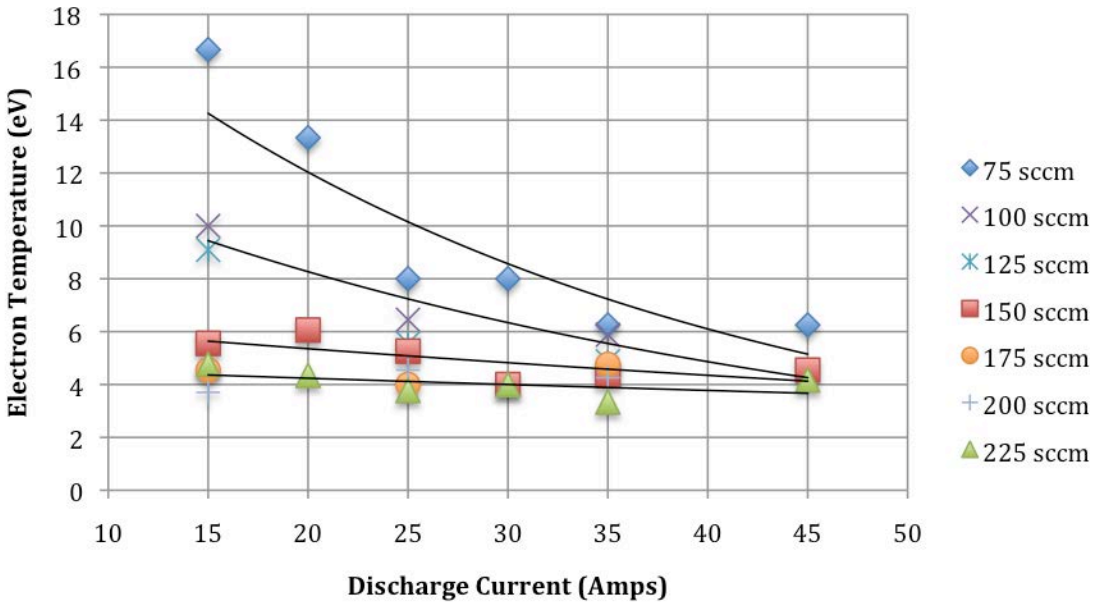

Figure 12. Electron temperature vs. discharge current

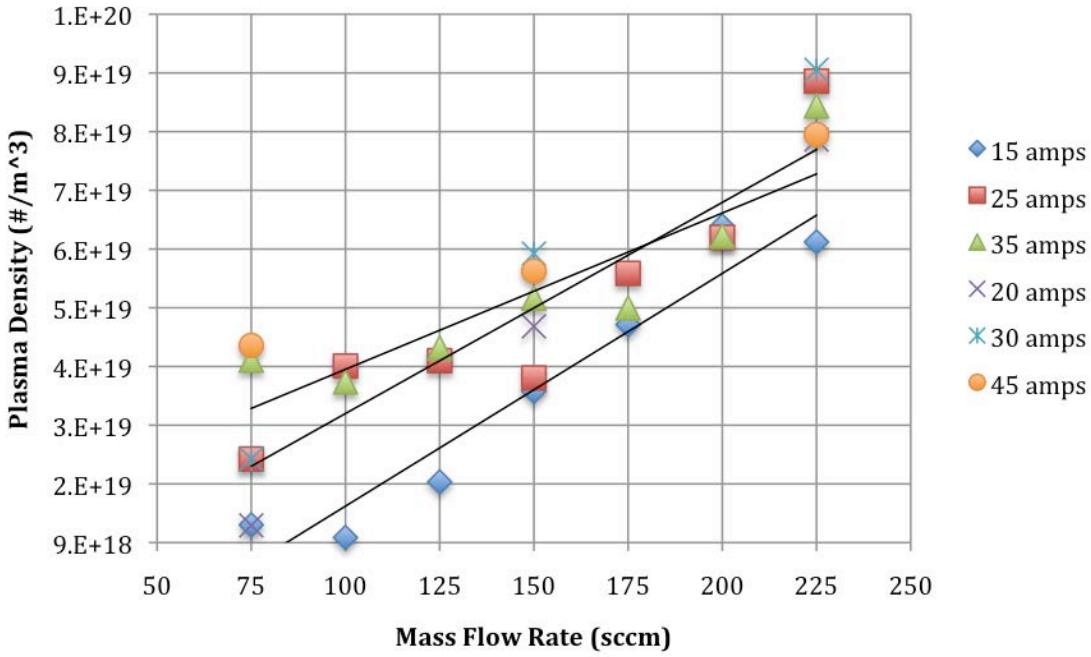

Figure 13. Plasma density vs. mass flow rate, at cathode exit plane.

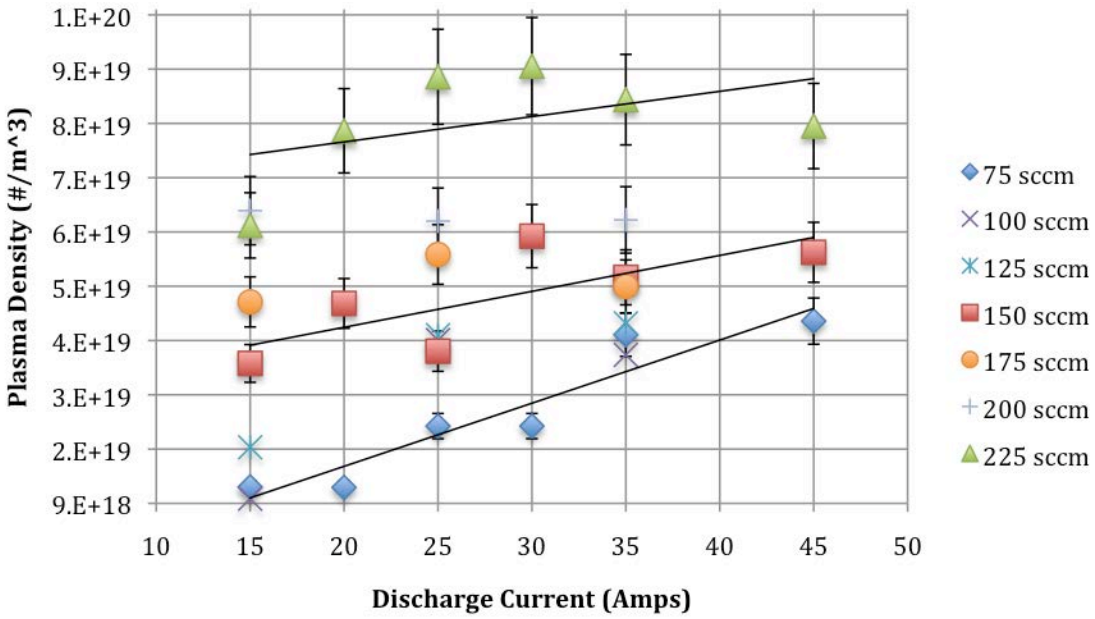

Figure 14. Plasma density vs. discharge current at cathode exit plane

Consider flow rates to the right of the minimum seen in the voltage vs. flow rate data. From the reported data it is seen that raising the mass flow rate corresponds to increasing discharge voltage and plasma density, and a decreasing electron temperature and active zone width. Increasing the flow rate will increase the density of neutrals inside the cathode, which increases the electron neutral collision frequency. The increased collision rate transfers energy from the electron stream to the neutrals, largely through inelastic collisions as verified by the increase in plasma density, thus lowering the electron temperature (inelastic collisions transfer very little energy between electrons and the much more massive neutrals). Energy is carried away from the discharge by these excited neutrals. Increasing the neutral density will decrease the likelihood of any one particular excited neutral colliding with an energetic electron, thus the stepwise ionization rate would decrease, requiring an increase in direct impact ionization from high-energy electrons. Compensation for this is seen by the discharge voltage increasing, thereby increasing the number of high-energy electrons. The processes reducing the electron energy are dominant over the increase in energy gained from the additional sheath drop, resulting in an overall decrease in average electron temperatures as measured.

Work on solid rod cathodes [8] reported electron temperatures in the discharge quite a bit lower than those presented here, though the solid rod work was at higher flow rates and much higher current levels. The data presented here does confirm that increasing both the discharge current and mass flow rate will decrease the electron temperature of the discharge plasma. Thus the discrepancy in measurements of the hollow cathode and the solid rod cathode discharge plasma electron temperature is supported by these trends.

III. Conclusions

Work on high current single channel hollow cathodes was recently completed at the University of Southern California's Astronautics and Space Technology Division. This work focused on the effects that varying discharge currents and interior cathode gas density had upon the cathode temperature distribution, the downstream plasma properties, and the behavior of the cathode active zone. This work provides connections to the behavior of SCHC's, solid rod cathodes, and traditional orificed hollow cathodes.

Of particular significance is the data indicating that the peak cathode temperature is a function of the mass flow rate, which is in disagreement with previous similar research. Additionally, a qualitative analysis of the behavior of the active zone was performed, demonstrating its dependence upon both the discharge current, and the mass flow rate. These trends indicate that the cathode temperature, and therefore material erosion rates, can be controlled by manipulation of the interior cathode gas density. Lower interior gas densities appear to promote conditions likely to increase the lifetime of these cathodes.

References

1. Giuliano, Downey, Erwin, "Design of High Current Hollow Cathode Test Facility", JPC-2007.
2. R. Downey, "Theoretical and Experimental Investigation of High Current Single Channel Hollow Cathode Arc Attachment". Ph.D. dissertation, University of Southern California, December 2008.

3. I. Mikellides, I. Katz, D. Goebel, J. Polk, "Theoretical Model of a Hollow Cathode Insert Plasma". AIAA 2004-3817.

4. I. Mikellides, I. Katz, D. Goebel, J. Polk, "Theoretical Model of a Hollow Cathode Plasma for the Assessment of Insert and Keeper Lifetimes". AIAA 2005-4234.

5. L. Cassady, "lithium-Fed Arc Multichannel and Single-Channel Hollow Cathode: Experiment and Theory". Ph.D. dissertation, Princeton University, September 2006.

6. L. Cassady, E. Choueiri. "Experimental and Theoretical Studies of the lithium-fed Multichannel and Single-channel Hollow Cathode". International Electric Propulsion Conference-2005-094.

7. J. Polk, "Mechanisms of Cathode Erosion in Plasma Thrusters". Ph.D. thesis, Princeton University, June 1995.

8. K.D. Goodfellow. "A Theoretical and Experimental Investigation of Cathode Processes In Electric Thrusters". Ph.D. dissertation, University of Southern California, May 1996.